Supplement to: Modulation of Intracortical Synaptic Potentials by Presynaptic Somatic Membrane Potential

Yousheng Shu, Andrea Hasenstaub, Alvaro Duque, Yuguo Yu, & David A. McCormick*

Contents: Supplementary Introduction; Supplementary Methods; Supplementary Results and Figures (Supplementary 1-8); Supplementary References

Supplementary Introduction

It is not possible for us to provide a comprehensive review of the vast literature on the electrophysiology of synaptic transmission, although for a general overview we recommend several reviews[5-9]. We provide here only a brief background for the non-specialist in order to clarify the contribution of our findings to the field of mammalian and intracortical synaptic transmission.

Synaptic transmission is traditionally classified into two distinct types: graded and action potential dependent. Graded transmission does not require the generation of action potentials, but rather operates through tonic synaptic vesicle release, the rate of which is modified by changes in the membrane potential of the presynaptic terminal (for review see[5,6,8,9,12]). Graded transmission is found at specific synaptic contacts in a wide variety of invertebrate nervous systems (e.g. see[13-18]), while in the vertebrate nervous system, graded transmission is believed to occur mainly at retinal photoreceptors and some retinal interneurons, in auditory hair cells of the cochlea, and in electroreceptors of the lateral line organ in fish and amphibians (see[6-9]). Graded transmission is believed to be particularly important for connections that require a tonic and high level of synaptic transmission, and where the cellular region of input (e.g. photoreceptors; mechanoreceptors) are not distant to the region of neurotransmitter release. At the vast majority of the remaining synaptic contacts, particularly in the mammalian nervous system, synaptic transmission is thought to occur through action potential-dependent triggered release. This action potential-dependent release has typically been treated as the main or even sole mechanism of synaptic information transmission from the presynaptic to postsynaptic neuron.

These two types of synaptic transmission may not be completely distinct. Several invertebrate synaptic connections exhibit both graded and action potential-dependent release, meaning that depolarization of the presynaptic cell may cause substantial release of transmitter onto the postsynaptic neuron without the generation of action potentials (e.g. graded release), but that the presynaptic neuron may also generate action potentials, which can also release transmitter (triggered release)[19-22]. Yet another hybrid form of synaptic transmission occurs in some invertebrate synaptic connections and is characterized by a change in the amplitude of the synaptic response evoked in the postsynaptic cell by a change in the membrane potential of the presynaptic neuron[13,15-18]. In these cases, it is believed that the synaptic release sites are sufficiently electrotonically close to the presynaptic soma to be affected by changes in somatic membrane potential, or that changes in membrane potential have a significant effect on the amplitude and/or duration of the action potentials that invade the presynaptic terminal. Available evidence indicates that enhancement of action potential triggered postsynaptic potentials in invertebrate preparations by depolarization of the presynaptic soma results from an increase in the probability of transmitter release[16], perhaps through increases in tonic levels of Ca^{2+} in the presynaptic terminals[23] or through broadening of presynaptic action potentials[18,24].

As in invertebrate preparations[18,24-27], the amplitude of action potential-evoked postsynaptic potentials in mammalian systems is strongly dependent upon the amplitude/duration of action potentials in the presynaptic terminal[28-34], as well as the steady membrane potential of the terminal[14]. Indeed, at the Calyx of Held, a synaptic terminal that is large enough to be patched and manipulated with whole cell recording electrodes, the amplitude of action potential-triggered synaptic potentials increases by approximately 10% per mV of depolarization of the presynaptic terminal, apparently owing to small increases in background Ca^{2+} levels associated with these tonic depolarizations[14]. Increases in concentration of Ca^{2+} in the synaptic terminal can enhance the probability of spike triggered release of synaptic vesicles[35-37], although the precise mechanisms by which very low increases in $[Ca^{2+}]_i$ may achieve this are not yet known. Changes in action potential duration in presynaptic terminals occur naturally during repetitive discharge and is likely an important mechanism for frequency-dependent enhancement of transmitter release[28,30,31,34]. These results are consistent with the general view that the amplitude of synaptic events evoked by invasion of the synaptic terminal by an action potential is strongly dependent upon the membrane potential, action potential duration, and/or resting Ca^{2+} concentrations of that terminal.

This property of synaptic transmission may be important for a variety of neuronal cell types in the mammalian brain. We hypothesize that it may be particularly relevant to the

*Department of Neurobiology, Kavli Institute for Neuroscience, Yale University School of Medicine, 333 Cedar Street New Haven, CT 06510 www.mccormicklab.org

operation of the cerebral cortex. In the cerebral cortex the axons of many cell types, both excitatory and inhibitory, form a relatively dense cloud of connections within the local neuronal network, in addition to more long range connections [1,38-44]. How electronically[arh1] close synaptic connections are to the parent soma in the neocortex has not been widely studied, nor has the effect of somatic membrane potential on the amplitude-duration of axonal action potentials. The possibility that changes in the membrane potential of presynaptic neuronal cell bodies may affect the amplitude of action potential-evoked postsynaptic potentials has not, to our knowledge, been previously investigated in the mammalian brain, although in culture systems it has been shown that axonal conduction failures may control the properties of intracortical synaptic communication[28,45,46](see however[47,48]). This lack of information results in large part from the technical challenge of performing simultaneous whole cell recordings from distal axons and their parent somata in mammalian systems.

Our study asked three simple questions: 1) Is the amplitude of synaptic potentials evoked by action potentials sensitive to the membrane potential at the cell body of the presynaptic neuron? 2) Do changes in the membrane potential of cortical neuronal somata propagate sufficient distances along their axons to cause a significant change in membrane potential of local presynaptic terminals? 3) Do changes in the membrane potential of presynaptic neurons have an effect on the amplitude and duration of axonal action potentials that is sufficiently large to alter the amplitude of synaptic potentials? Through the investigation of synaptic transmission between pairs of layer 5 pyramidal cells maintained in slices in vitro, we answer all three of these questions. First, we demonstrated that the amplitude of action potential evoked EPSPs between synaptically connected pairs of pyramidal cells is a continual function of membrane potential at the soma of the presynaptic neuron. Next, through the simultaneous whole cell patch clamping of pyramidal cell bodies and their distal axons, we demonstrate that membrane potential changes and synaptic barrages propagate sufficiently far down these axons to have a significant effect on the membrane potential of at least nearby synaptic terminals. Finally, we show that changes in membrane potential at the cell body have a significant effect on the duration/amplitude/area of axonal action potentials, even several hundred microns distant.

Thus, we demonstrate that information transmission between neurons in the cerebral cortex is not limited to the rate and timing of action potentials propagating down the axons, but rather, at least for synapses that are electrotonically close to the soma, information transfer may also directly utilize the voltage-time course of the membrane potential of the presynaptic neuron (although our studies of the kinetics of the facilitatory response suggest that there may be a limitation in the frequency transfer ability of this mechanism) either through a direct depolarization of presynaptic terminals and/or through changes in axonal action potential waveform. These results suggest that synaptic transmission in the mammalian brain, as in invertebrates, may often operate in a regime that is best considered as action potential-triggered release that is graded by presynaptic somatic membrane potential and opens the possibility that information transmission in the brain is far more efficient than previously appreciated.

Supplementary Methods

Obtaining whole cell recordings from the cut ends of cortical axons

Whole-cell recordings were achieved from both soma and the cut end of the main axon using a Multiclamp 700B or Axoclamp 2B amplifier (Axon Instruments, Union City, CA). Patch pipettes were formed on a Sutter Instruments (Novato, CA) P-97 microelectrode puller from borosilicate glass (1B200-4, WPI, Sarasota, FL). Pipettes for somatic recording had an impedance of 5-6 MΩ, and were filled with an intracellular solution that contained (in mM): KGluconate 140, KCl 3, $MgCl_2$ 2, Na_2ATP 2, HEPES 10, pH 7.2 with KOH (288 mOsm). Calcium buffers included in the whole cell pipette were 0.2 mM EGTA for axonal recordings and either 1 or 10 mM EGTA or 0.025 mM BAPTA for recording from synaptically connected pairs of pyramidal cells, as stated in the main text. Alexa Fluo 488 (100 μM; for axonal recording experiments only) and biocytin (0.2%) were added to the pipette solution for tracing and labeling the recorded pyramidal cells. For simultaneous somatic and axonal whole cell recordings, approximately 5 minutes after somatic whole-cell recording was established, the course of the main axon was examined under the fluorescent microscope (Zeiss Axioskop 2 FS Plus) equipped with a 40x water immersion objective and a magnifier of up to 2x. Only those pyramidal neurons in which the axon was at least 60 μm in length and came to the upper surface of the slice were used in this portion of our study. Patch pipettes for whole cell axonal recording were filled with a similar intracellular solution, but without fluorescent dye added; these had an impedance of 9-15 MΩ. The pipette was advanced to the cut end of the axon with a positive pressure of about 65 mbar, and guided by switching back and forth between the fluorescent and DIC images of the axon, with the total time the cell was exposed to fluorescence being kept to less than 20 seconds to minimize damage (our whole cell recordings from the soma did not reveal any evidence of changes in the electrophysiological properties of the recorded neurons during this brief exposure to fluorescence). The bleb formed at the end of the axon was then pressed by the pipette tip and negative pressure was applied to form a seal. As soon as a tight seal (>10 GΩ) was achieved, pulses of brief suction were applied to break the patch, and the whole-cell configuration could be easily

*Department of Neurobiology, Kavli Institute for Neuroscience, Yale University School of Medicine, 333 Cedar Street New Haven, CT 06510 www.mccormicklab.org

obtained. Thereafter, steps of positive current and negative current were injected to the soma and axon to examine the intrinsic membrane properties of the recorded neuron. During the whole period of simultaneous somatic and axonal recordings, access resistance was monitored frequently; recordings with access resistance higher than 25 MΩ for somatic recording, 45 MΩ for axonal recording, were discarded. Bridge balance and capacitance neutralization were carefully adjusted before and after every experimental protocol. After a recording was completed, the slice was transferred to 4% paraformaldehyde in 0.1 M phosphate buffer for subsequent immunostaining and visualization.

Calculation of Transfer Function from Soma to Axon

All computations were performed in Spike2 (Cambridge Electronic Design, Cambridge, UK) and MATLAB (MathWorks, Bethesda, MD). Continuous frequency transfer functions for the axon were examined through the injection of conductance noise with a dynamic clamp technique[49] and estimated using Welch's averaged periodogram method. Discrete frequency transfer functions for the axon were estimated using Wiener's method.

Measurements of Spike Parameters

The duration, amplitude, and area of action potentials were measured by first determining the point of spike baseline. This was achieved through examination of dV/dt of the action potential and determining the point at which dV/dt approached 0 after the falling phase of the action potential. Action potential amplitude was determined by the difference between the spike peak and the spike baseline, while duration was measured at half spike amplitude. Area was measured as the integrated amplitude-time course between the spike and the baseline. Similar results were also obtained if we used spike threshold as the baseline or if we measured spike width at base.

Obtaining slow oscillations in submerged cortical slices

The slow oscillation is a recurrent network activity occurring in vivo during periods of slow wave sleep[50]. This oscillation is also robustly observed in slices of ferret cortex maintained in the interface chamber in vitro, when the concentrations of Ca^{2+} and Mg^{2+} in the bathing medium are reduced to 1 mM each, while the level of K^{+} is increased to 3.5 mM; values that are closer to their natural levels in situ [51]. To obtain the slow oscillation in the submerged chamber (manuscript Figure 4a), we found it necessary to suspend the slice between two grids so that the ACSF solution flowed freely over as well as under the cortical slice. Presumably this increased delivery of oxygen to the cortical slice is important for maintaining a sufficiently healthy network for generation of this recurrent cortical activity.

*Department of Neurobiology, Kavli Institute for Neuroscience, Yale University School of Medicine, 333 Cedar Street New Haven, CT 06510 www.mccormicklab.org

Supplemental Results and Figures

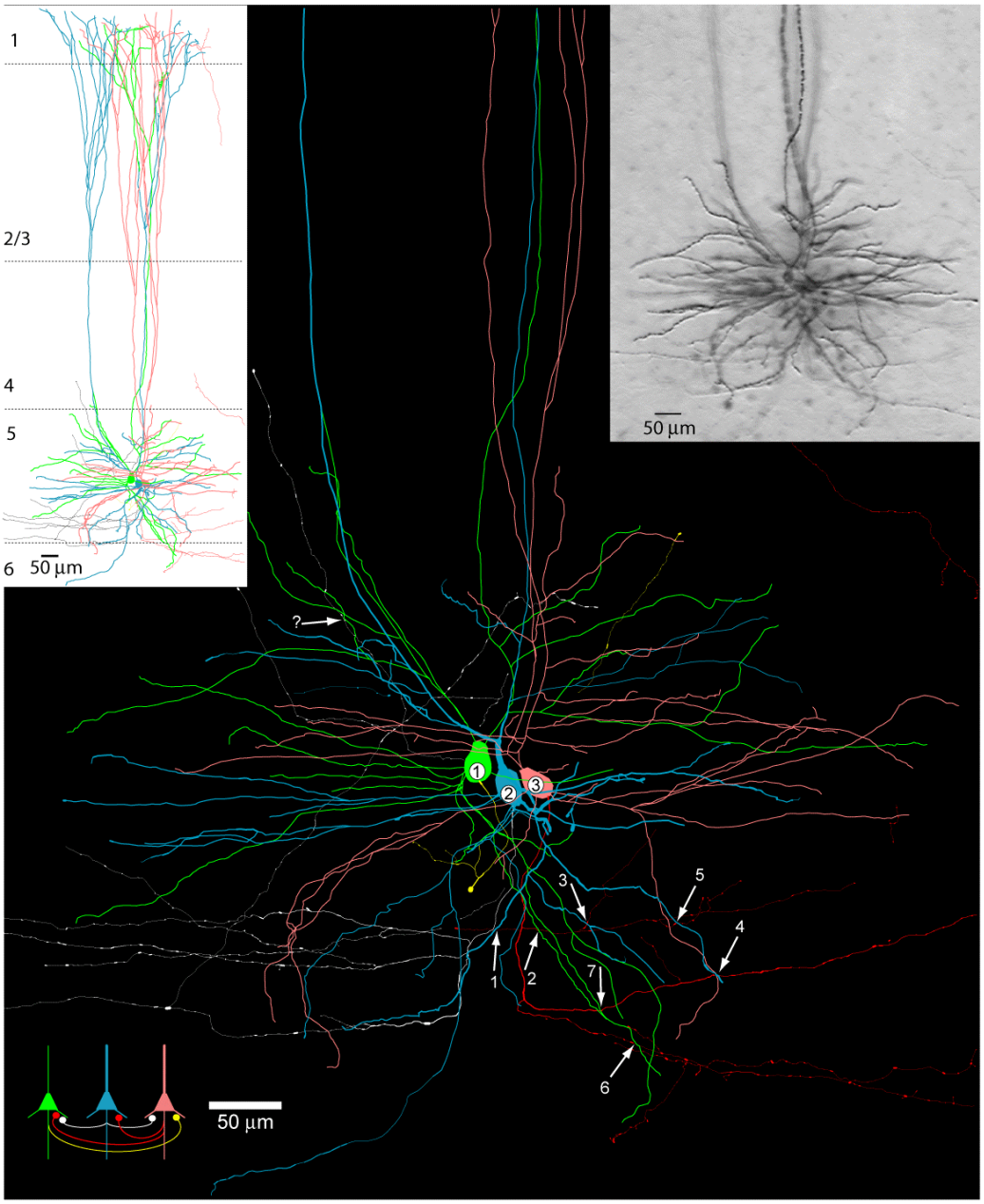

Supplementary Figure 1. Layer 5 pyramidal cells are interconnected by several synaptic boutons that are within one length constant of the axon. Simultaneous patch clamp recording from three layer 5 pyramidal neurons revealed synaptic connections as illustrated in the lower left schematic. Anatomical reconstruction in 3-D of the three biocytin filled neurons, using Neurolucida, indicated several putative synaptic boutons (white arrows), mostly on the basal dendrites. Three of these putative connections (white arrows 1, 3, 5) from cell 3 (red axon) onto cell 2 (blue dendrites) are found at 123, 154, 210 µm from the axon root. Another three (white arrows 2, 6, 7) from cell 3 (red axon) onto cell 1 (green dendrites) are found at 116, 258, 213 µm away from the axon root (see also[42]). One putative autapse of cell 3 (white arrow 4) is also found at 306 µm from the axon root. Cells were filled with biocytin and visualized with Ni-Co enhanced DAB. The tissue was covered-slipped but preserved wet in aqueous mounting media. Shrinkage correction (5%) was applied for the thickness (z-axis) only. The cells were reconstructed (63 to 157.5 magnification), in Neurolucida v. 6 interfaced to a Zeiss Axioskop microscope using a 63 water immersion lens. Morphometric data was obtained using Neurolucida Explorer v.4.50.3. The results presented in Figure 1b of the paper were obtained from the connection between cells 3 (pre) and 1 (post). Not all branches of the basal dendrites are illustrated for clarity.

*Department of Neurobiology, Kavli Institute for Neuroscience, Yale University School of Medicine, 333 Cedar Street New Haven, CT 06510 www.mccormicklab.org

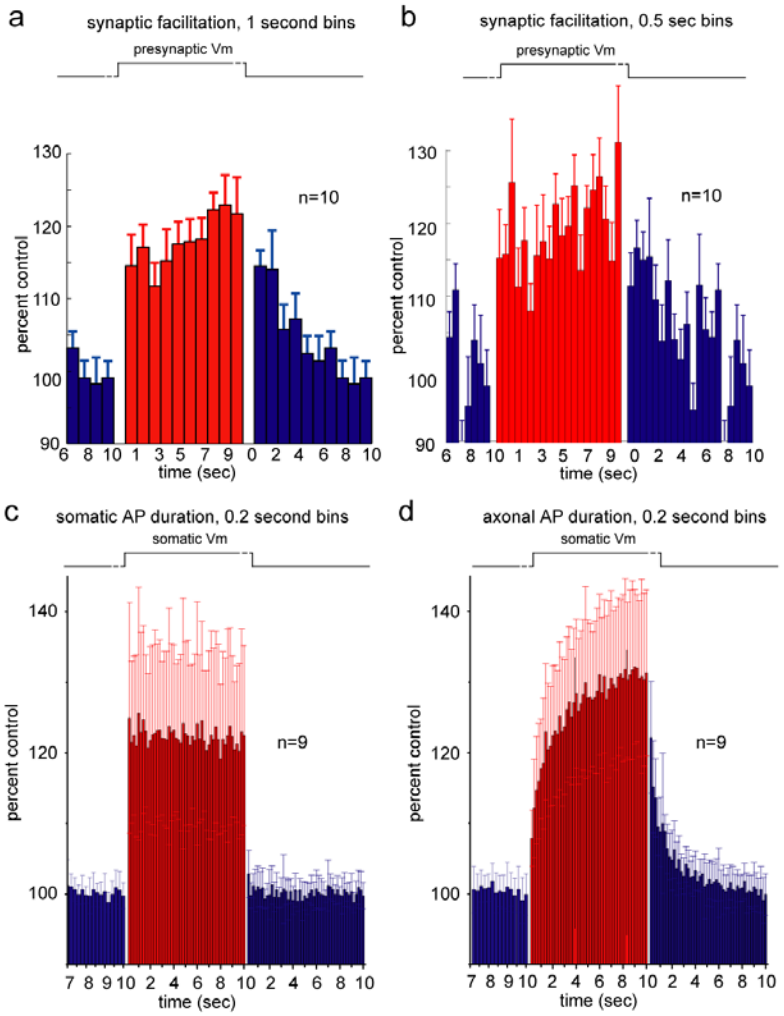

Supplementary Figure 2. Time course of synaptic facilitation and action potential broadening at increased time resolution. a. Reproduction of the plot from Figure 1f of the manuscript, in which the percent EPSP facilitation and disfacilitation is plotted with 1 second time bins. Red bars are during depolarization of the presynaptic neuron, while blue bars show periods when the presynaptic cell is at rest. All the bars during the facilitation period are significantly larger than those of the last 4 seconds of the hyperpolarized period. Additionally, there was a statistically significant trend for the facilitation to become larger over the 10 seconds of presynaptic depolarization, as indicated by a significant Spearman's rank correlation ($p<0.05$). b. Plot of the same data as in a, except with bin widths of 0.5 sec. The results are the same, but the decreased bin width increases variance. c. Relative increase in spike duration at the soma following depolarization, plotted with 0.2 sec bins. Note the rapid change in spike duration at the soma. d. Plot of relative increase in spike duration in the distal (average of 215 μm) axon following depolarization of the soma, at 0.2 sec bin width resolution. Mean and SEM are plotted. The SEM of individual cells was much smaller than that for the group data, owing to differences between cells in the percentage of change in action potential duration. On each trial, EPSPs or spikes were evoked at 0.8 to 1 Hz, but the timing was varied between trials so as to change the relationship between the onset of somatic depolarization and spike initiation.

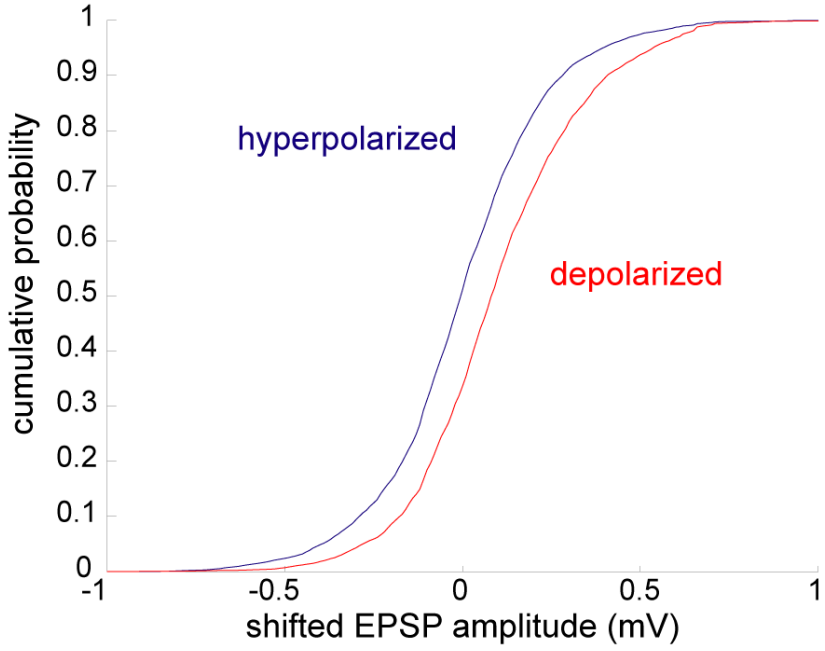

Supplementary Figure 3. Normalized cumulative probability of EPSP amplitude when the presynaptic cell is at rest (hyperpolarized; blue) or following depolarization by 10-15 mV (depolarized; red). The cumulative histogram is the proportion of the EPSPs that were smaller than the amplitude on the x-axis, with one being the full distribution. The cumulative distribution was normalized for each cell by subtracting off the average EPSP amplitude at 0.5 cumulative probability (that is, the median EPSP size) for the hyperpolarized condition (thus making this value 0). The traces from the individual cell pairs (n=15) were then averaged. The average EPSP amplitude in our sample was 0.48 mV.

*Department of Neurobiology, Kavli Institute for Neuroscience, Yale University School of Medicine, 333 Cedar Street New Haven, CT 06510 www.mccormicklab.org

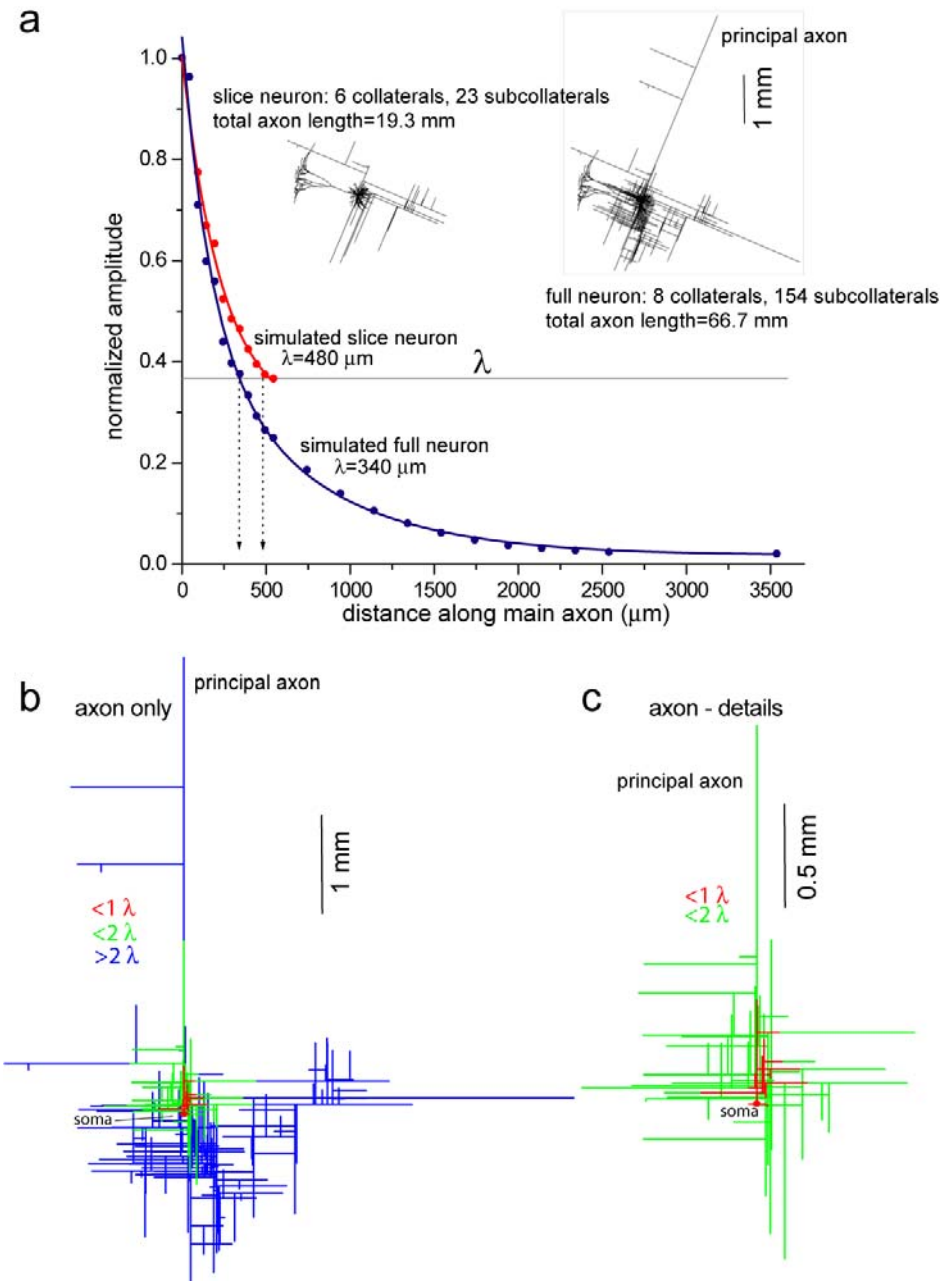

Supplementary Figure 4. Computational model of the length constant of the principal axon for cortical neurons.

a. Measurement of the length constant of a modeled axonal arbor that either preserves the connectivity observed in cortical slices (slice neuron) or is more complete (full neuron). The model "slice neuron" layer 5 pyramidal cell was endowed with an axon that had one principal axon that gave rise to 6 collateral and 22 subcollaterals, based upon the numbers of collaterals and subcollaterals observed in layer 5 pyramidal cells in our slices (n=14 cells). The length constant λ of the main axon under these conditions was 480 µm. Increasing the number of collaterals and subcollaterals as per the electrotonic structure of the axonal arbor of a fully reconstructed layer 5 neuron in vivo [Figure 2c in Binzegger et al.[1]], yielded a principal axon length constant that was reduced to 340 µm. **b**. Calculation of the regions of the axonal arbor in which the decay of voltage from the soma is within 1/e (1 λ; red), and $1/e^2$ (2 λ; green), or greater than $1/e^2$ (2 λ; blue) distant from the cell body. **c**. Expansion of the region of the modeled axonal arbor that is within 1 λ (red) and 2 λ (green) of the cell body. The total axonal length within 1 λ of the cell body is 1720 µm and within 2 λ is 12.5 mm. Given an average bouton density of one bouton per 8-12 µm[4], this would yield between 144 and 219 presynaptic boutons within 1 λ and 1042 to 1562 boutons within 2 λ of the cell body. Computational models of a second axonal branching pattern based upon the axonal arbor of a cortical layer 2/3 pyramidal cell [Figure 2A in Binzegger et al.[1]] yielded similar results (1860 µm within 1 λ and 13.5 mm within 2 λ). Based on cable theory, the length constant λ is mainly determined by $\lambda \propto \sqrt{DR_m / R_i}$ where D is diameter of the axon, R_m is membrane resistance and R_i is axial resistance. Our simulation confirmed the importance of these variables (see also[11]).

*Department of Neurobiology, Kavli Institute for Neuroscience, Yale University School of Medicine, 333 Cedar Street New Haven, CT 06510 www.mccormicklab.org

Model Methods: Our computational model was implemented using NEURON 5.8[7] and utilized the published multi-compartmental model of the full dendritic and somatic structure of a layer 5 cortical pyramidal cell (Figure 1D in Mainen and Sejnowki[52]) coupled together with a reconstruction of cortical pyramidal cell axons according to Binzegger et al.[1]. The temperature of the modeled cell was 37^{o} C.

Dendrites and soma The soma and dendrites contain 164 segments. The somatic surface area is 2,748 μm^2, while its diameter is 25 μm, and its length is 35 μm. There are 11 primary neurites, 87 branches, totaling 17,667.6 μm in length and 78,858 μm^2 in surface area.

Axon Our model of the axon began with that of Mainen et al.[53], and was subsequently modified to include either a reduced axonal arbor that was of similar length and branching pattern as that of our biocytin-filled neurons in vitro, or a more complete axonal arbor modeled after that of Binzegger et al.[1]. In addition, we modified membrane capacitance and ionic conductances in order to match the frequency-dependent transfer of membrane potential from the soma down the main axon (see Supplementary Figure 6 below).

Main axon: The soma connects to the axon hillock, which is the transitional zone between the soma and initial segment proper. The width of various axonal components were matched to those that we measured in our recorded neurons (e.g. see Figure 1). The axon hillock tapers from 2.8 μm to 0.92 μm and has a length of 5 μm. The hillock is followed by a 40 μm initial segment of 0.92 μm diameter. Following the initial segment, there is a 500 μm length of unmyelined axon (0.83 μm in diameter), since in our examinations, the main axons of prefrontal cortical neurons in 2 month old ferrets only became myelinated at approximately this distance (Alvaro Duque, unpublished observations). The next portion of the main axon is myelinated and 3000 μm in length, with internode distances of 200 μm. We assumed an internode diameter of 0.46 μm and node diameter and length of 0.92 μm. Internodes are modeled as 75 segments and nodes are a single segment.

Axon collaterals of full layer 5 pyramidal cell: After Binzegger et al.[1], we reconstructed a model of an axonal arbor of a layer 5 pyramidal cell consisting of 196 segments composed of 10,026 compartments total. All collaterals were assumed to be unmyelinated. There are 8 first order collaterals (diameter 0.55 μm), 23 second order collaterals (diameter 0.37 μm), and 131 third, forth and fifth order collaterals (diameter 0.37 μm). The total length of collaterals is approximately 64 mm. Including the main axon, the total axon length is 66.7 mm.

Axon collaterals of "slice" layer 5 pyramidal cell: For the slice neuron simulation, the dendritic tree and soma are the same as in the simulated full neuron, but there are 6 first order collaterals, 22 second order collaterals, totaling 18.7 mm in length consisting of 35 sections composed of 3,293 compartments. With the main axon, the total axonal length for the slice neuron is 19.2 mm.

Electrical properties The membrane capacitance Cm for the soma, dendrites, and unmyelinated axon is modeled as 0.75 μF /cm^2. The axial resistance for dendrite and axon is 90 Ω-cm.[52] The capacitance of the myelinated axon is much lower and is Cm=0.04 μF /cm^2. The capacitance for the unmyelinated axon is 0.4 and for collaterals 0.24 μF /cm^2 which is according to the experimental data (see Supplemental Figure 6 below). The membrane time constant of the soma, dendrite, hillock and initial segment is 12 msec, while for the main axon and collaterals it lies in a range from 3 to 7 msec according to the experimental data.

Channel distributions: The transient Na^+ current is present in all parts of the modeled cell and its density is high in the initial segment, hillock and node (30,000 pS/μm^2), but low in the soma (2000 pS/μm^2) and dendrites (20 pS/μm^2). In unmyelinated model axon and collaterals, Na^+ conductance is between 300-1000 pS/μm^2 (the thinner the collateral, the lower the value of the Na conductance). Myelinated model axon has a low Na^+ conductance value of 20 pS/μm^2. The reversal potential of Na^+ in our model is 60 mV.

The fast, voltage activated K^+ current, I_{Kv} is present in the model hillock, initial segment, and node (2000 pS/μm^2). The density is lower for soma (1000 pS/μm^2), axon collaterals (50 pS/μm^2 for 1st, 20 for 2nd order collaterals, 10 for higher order collaterals). The reversal potential of K^+ is -90 mV. These changes were made to match the experimental recording and keep the spike propagation stable.

The slow non-inactivating potassium current (M-current; I_{km}), high-voltage activated Ca^{2+} current, I_{Ca} and one Ca^{2+} dependent K^+ current, $I_{kCa,}$ are distributed throughout the soma and dendrites (Km conductance 0.1, Ca conductance 0.3, and Kca conductance is 3 pS/μm^2) as per Mainen et al.[52]. The reversal potential of Ca is 140 mV.

Background leak current is distributed throughout the cell. In the soma, dendrites, hillock, initial segments, unmyelinated axon and collaterals, gleak = 0.0000667 S/cm^2. In the nodes, gleak = 0.02 S/cm^2, and in the myelinated axon, gleak= 0.00002 S/cm^2. The reversal potential of the leak current is -70 mV.

For the specific rate functions for the different ionic channels please see Mainen et al.[52].

*Department of Neurobiology, Kavli Institute for Neuroscience, Yale University School of Medicine, 333 Cedar Street New Haven, CT 06510 www.mccormicklab.org

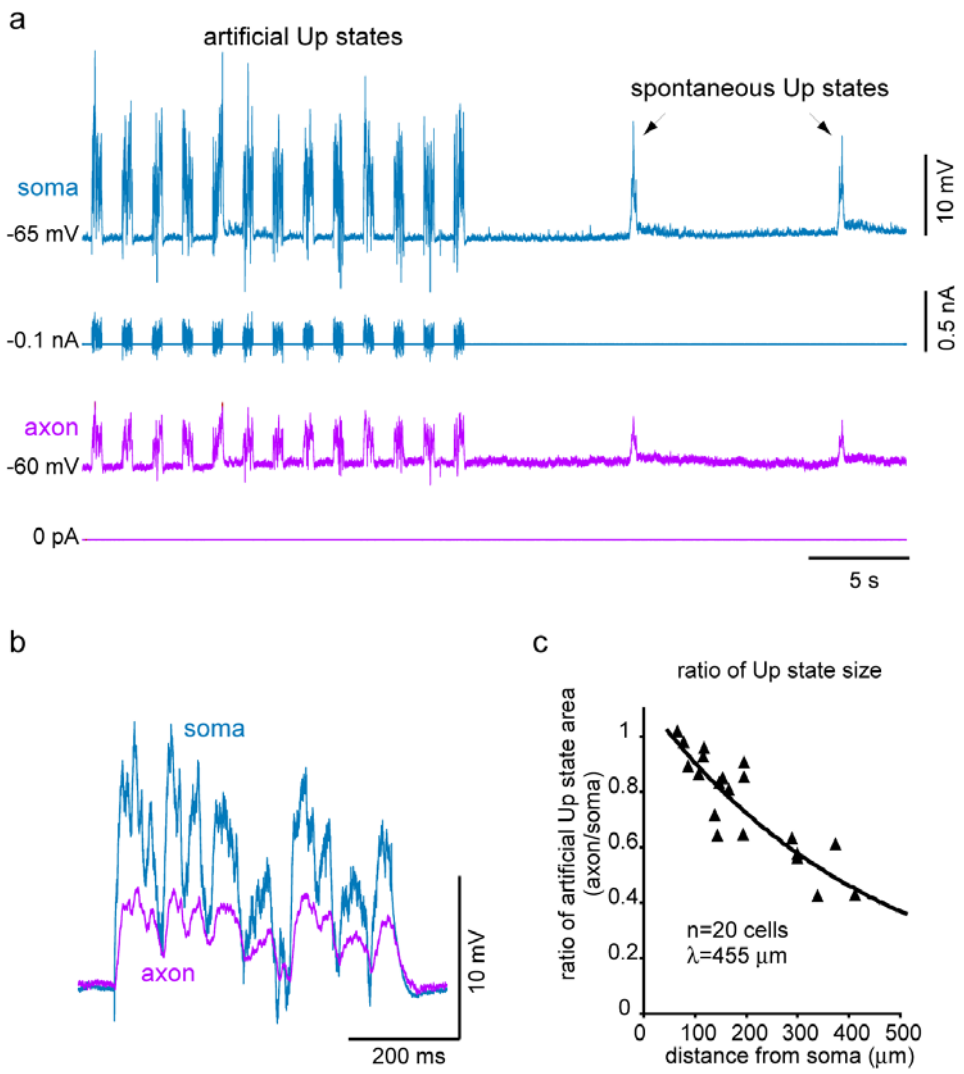

Supplementary Figure 5. Artificial barrages of synaptic activity propagate over significant distances down the main axon.

a. Artificial Up states, consisting of a combined excitatory and inhibitory noisy conductance model[2,3], were injected into the soma, while simultaneously recording from the soma and cut end of the main axon (180 µm distant). Two spontaneous Up states occurred after the cessation of somatic current injection. **b**. Overlay of the somatic and axonal membrane responses to the artificial somatic Up state. **c**.. Calculation of the length constant of the axon for artificial synaptic activity yields a result (455 µm) similar to that calculated with naturally occurring spontaneous synaptic barrages. These experiments were performed with the dynamic clamp technique using a DAP-5216a board (Microstar Laboratory). Noisy conductances were constructed according to an Ornstein-Uhlenhbeck (colored noise) model[10].

*Department of Neurobiology, Kavli Institute for Neuroscience, Yale University School of Medicine, 333 Cedar Street New Haven, CT 06510 www.mccormicklab.org

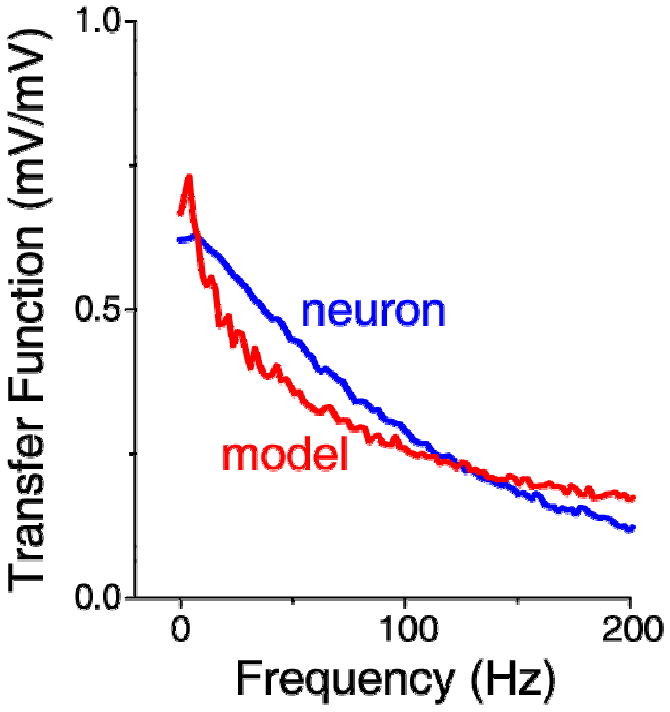

Supplementary Figure 6. Transfer of somatic conductance to axonal voltage is frequency dependent. A noisy excitatory conductance was injected with a dynamic clamp system into the soma and the resulting somatic current and somatic voltage change, along with the axonal voltage change (162 µm from soma), were then recorded. Calculation of somatic to axonal voltage transfer yields a strongly frequency dependent function (blue line, neuron). Overlaid for comparison is the transfer function calculated for our model pyramidal cell with the reduced axonal arbor typical of neurons in the slice (see Supplementary Figure 3). The model was adjusted to so that its axonal transfer function provided a reasonable fit for cortical pyramidal cells.

Methods: In the real neuron, the standard deviation (and, concurrently, the amplitude) of the injected conductance was adjusted to give a 10 mV peak-to-peak membrane potential deviation, and the holding current was adjusted to keep the cell just below spike threshold. The transfer function from the injected conductance to the recorded membrane potential fluctuations was then calculated using Wiener's method.

Passive properties of the axonal bleb. Whole cell, gigohm seal, recordings were simultaneously obtained from the cut end of the axon as well as the cell body of layer 5 pyramidal cells in the ferret prefrontal cortical slice in vitro. The resting membrane potential of these axonal recordings (recorded at an average distance of 158 µm from the soma) were on average –60.1 +/- 4.0 mV (n=13), which is similar to the resting membrane potential of the somata of the same neurons (-62.8 +/- 3.4 mV). The time constant of the axonal recordings was short (4.2 +/- 2.7 msec) and the input resistance was high (128.2 +/- 61.1 Megohms). Injection of subthreshold 500 msec duration hyperpolarizing and depolarizing current pulses revealed a relatively linear I-V relation (not shown). The spherical structure on the end of the axon is relatively small (a few microns in diameter) and therefore will be electronically close to undamaged axon. The action potential properties recorded from the sealed end of the axon should, therefore, be representative of action potentials in the axon.

*Department of Neurobiology, Kavli Institute for Neuroscience, Yale University School of Medicine, 333 Cedar Street New Haven, CT 06510 www.mccormicklab.org

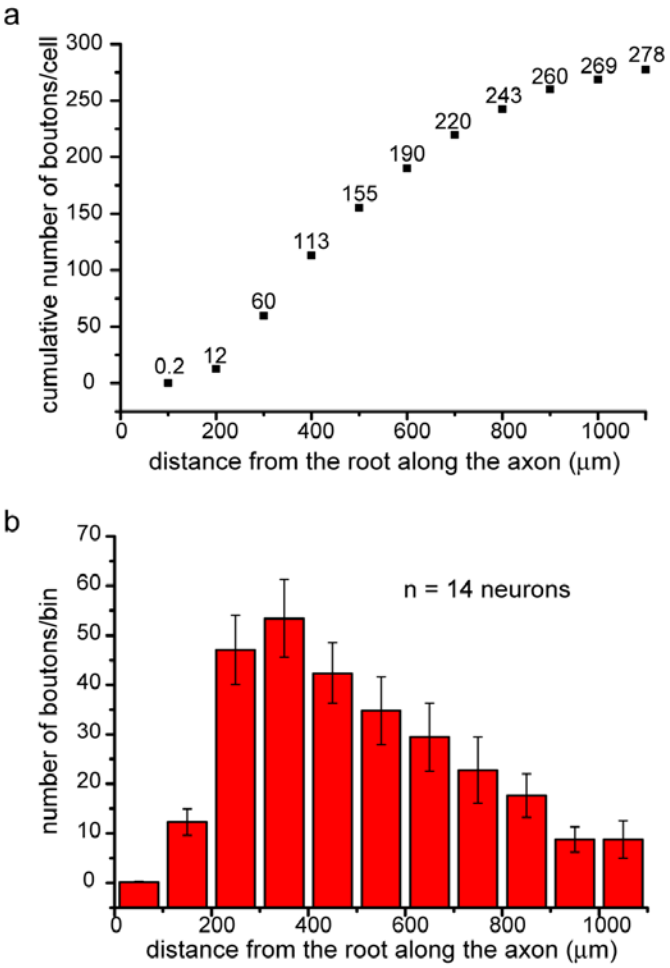

Supplementary Figure 7. Cortical pyramidal cells give rise to numerous nearby putative synaptic boutons. **a**. Cumulative number of putative boutons along the axon per cell (n=14 layer 5 pyramidal neurons) binned every 100 µm from the root. Numbers per data point indicate the average number of boutons found x distance away from the root. The root could be the soma (n=10) or a dendrite (n=4). **b**. Mean number of boutons per bin (bin size 100 µm) along the axon. Error bars are SEM. These numbers are likely an underestimate of the in vivo condition, since the main axon and sometimes axon collaterals were cut during slice preparation. In addition, the visualization of biocytin was performed without resectioning of the tissue, which allowed the axon to remain as intact as possible, but which increased the probability that portions of the axon were too lightly stained to detect boutons. See Supplementary Figure 1 for methods.

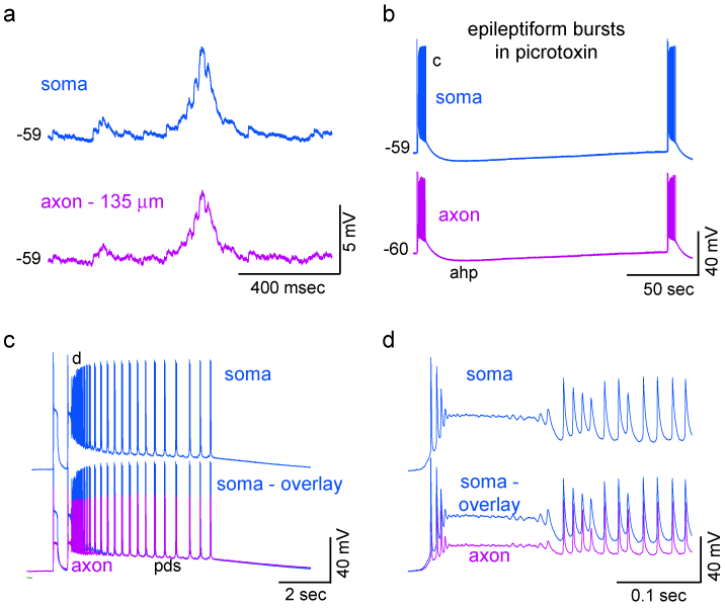

Supplementary Figure 8. Epileptiform activity propagates down the axon. **a**. Simultaneous somatic and axonal (135 µm from the soma) recording of spontaneous synaptic activity in a layer 5 pyramidal cell. Note that the waveform of barrages of synaptic activity propagates down the axon. **b**. Following the bath application of the $GABA_A$ receptor antagonist picrotoxin (50 µM), epileptiform bursts are generated within the slice. Note the similarity of the somatic and axon membrane potentials, even during the slow afterhyperpolarization (ahp) that follows each epileptiform burst. **c**. Expansion of an epileptiform burst. Although the amplitude of the initial plateau is smaller in the axon than in the soma (expanded in **d** for detail), the later portions of the paroxysmal depolarization shift (pds) are similar in the two recording sites. These results indicate that not only action potentials, but also the pronounced depolarizations, of epileptiform activity propagate along intracortical axons.

*Department of Neurobiology, Kavli Institute for Neuroscience, Yale University School of Medicine, 333 Cedar Street New Haven, CT 06510 www.mccormicklab.org

References

1. Binzegger, T., Douglas, R. J. & Martin, K. A. Axons in cat visual cortex are topologically self-similar. *Cereb Cortex* **15**, 152-65 (2005).
2. Ho, N. & Destexhe, A. Synaptic background activity enhances the responsiveness of neocortical pyramidal neurons. *J Neurophysiol* **84**, 1488-96 (2000).
3. Destexhe, A., Rudolph, M., Fellous, J. M. & Sejnowski, T. J. Fluctuating synaptic conductances recreate in vivo-like activity in neocortical neurons. *Neuroscience* **107**, 13-24 (2001).
4. Anderson, J. C., Binzegger, T., Douglas, R. J. & Martin, K. A. Chance or design? Some specific considerations concerning synaptic boutons in cat visual cortex. *J Neurocytol* **31**, 211-29 (2002).
5. Cowan, W. M., Sudhof, T.C., Stevens, C.F. *Synapses* (Johns Hopkins University Press, Baltimoare, 2001).
6. Juusola, M., French, A. S., Uusitalo, R. O. & Weckstrom, M. Information processing by graded-potential transmission through tonically active synapses. *Trends Neurosci* **19**, 292-7 (1996).
7. Lenzi, D. & von Gersdorff, H. Structure suggests function: the case for synaptic ribbons as exocytotic nanomachines. *Bioessays* **23**, 831-40 (2001).
8. Sterling, P. & Matthews, G. Structure and function of ribbon synapses. *Trends Neurosci* **28**, 20-9 (2005).
9. Wilson, M. Synaptic physiology: plenty of models to choose from. *Curr Biol* **14**, R666-7 (2004).
10. Shu, Y., Hasenstaub, A., Badoual, M., Bal, T. & McCormick, D. A. Barrages of synaptic activity control the gain and sensitivity of cortical neurons. *J Neurosci* **23**, 10388-401 (2003).
11. Rall, W. in *The Nervous System: Cell Biology of Neurons.* (ed. Kandel, E. R.) 39-97 (American Physiological Society, Bethesda, Maryland, 1977).
12. Jessell, T. M. & Kandel, E. R. Synaptic transmission: a bidirectional and self-modifiable form of cell-cell communication. *Cell* **72 Suppl**, 1-30 (1993).
13. Meyrand, P., Weimann, J. M. & Marder, E. Multiple axonal spike initiation zones in a motor neuron: serotonin activation. *J Neurosci* **12**, 2803-12 (1992).
14. Awatramani, G. B., Price, G. D. & Trussell, L. O. Modulation of transmitter release by presynaptic resting potential and background calcium levels. *Neuron* **48**, 109-21 (2005).
15. Nicholls, J. & Wallace, B. G. Modulation of transmission at an inhibitory synapse in the central nervous system of the leech. *J Physiol* **281**, 157-70 (1978).
16. Nicholls, J. & Wallace, B. G. Quantal analysis of transmitter release at an inhibitory synapse in the central nervous system of the leech. *J Physiol* **281**, 171-85 (1978).
17. Shimahara, T. & Tauc, L. Multiple interneuronal afferents to the giant cells in Aplysia. *J Physiol* **247**, 299-319 (1975).
18. Shapiro, E., Castellucci, V. F. & Kandel, E. R. Presynaptic membrane potential affects transmitter release in an identified neuron in Aplysia by modulating the Ca2+ and K+ currents. *Proc Natl Acad Sci U S A* **77**, 629-33 (1980).
19. Graubard, K., Raper, J. A. & Hartline, D. K. Graded synaptic transmission between identified spiking neurons. *J Neurophysiol* **50**, 508-21 (1983).
20. Graubard, K., Raper, J. A. & Hartline, D. K. Graded synaptic transmission between spiking neurons. *Proc Natl Acad Sci U S A* **77**, 3733-5 (1980).
21. Kristan, W. B., Jr., Calabrese, R. L. & Friesen, W. O. Neuronal control of leech behavior. *Prog Neurobiol* **76**, 279-327 (2005).
22. Manor, Y., Nadim, F., Abbott, L. F. & Marder, E. Temporal dynamics of graded synaptic transmission in the lobster stomatogastric ganglion. *J Neurosci* **17**, 5610-21 (1997).
23. Ivanov, A. I. & Calabrese, R. L. Modulation of spike-mediated synaptic transmission by presynaptic background Ca2+ in leech heart interneurons. *J Neurosci* **23**, 1206-18 (2003).
24. Byrne, J. H. & Kandel, E. R. Presynaptic facilitation revisited: state and time dependence. *J Neurosci* **16**, 425-35 (1996).
25. Augustine, G. J. Regulation of transmitter release at the squid giant synapse by presynaptic delayed rectifier potassium current. *J Physiol* **431**, 343-64 (1990).
26. Ma, M. & Koester, J. Consequences and mechanisms of spike broadening of R20 cells in Aplysia californica. *J Neurosci* **15**, 6720-34 (1995).
27. Ma, M. & Koester, J. The role of K+ currents in frequency-dependent spike broadening in Aplysia R20 neurons: a dynamic-clamp analysis. *J Neurosci* **16**, 4089-101 (1996).
28. Debanne, D. Information processing in the axon. *Nat Rev Neurosci* **5**, 304-16 (2004).
29. Borst, J. G. & Sakmann, B. Effect of changes in action potential shape on calcium currents and transmitter release in a calyx-type synapse of the rat auditory brainstem. *Philos Trans R Soc Lond B Biol Sci* **354**, 347-55 (1999).
30. Geiger, J. R. & Jonas, P. Dynamic control of presynaptic Ca(2+) inflow by fast-inactivating K(+) channels in hippocampal mossy fiber boutons. *Neuron* **28**, 927-39 (2000).
31. Jackson, M. B., Konnerth, A. & Augustine, G. J. Action potential broadening and frequency-dependent facilitation of calcium signals in pituitary nerve terminals. *Proc Natl Acad Sci U S A* **88**, 380-4 (1991).
32. Qian, J. & Saggau, P. Modulation of transmitter release by action potential duration at the hippocampal CA3-CA1 synapse. *J Neurophysiol* **81**, 288-98 (1999).
33. Wheeler, D. B., Randall, A. & Tsien, R. W. Changes in action potential duration alter reliance of excitatory synaptic transmission on multiple types of Ca2+ channels in rat hippocampus. *J Neurosci* **16**, 2226-37 (1996).
34. Sabatini, B. L. & Regehr, W. G. Control of neurotransmitter release by presynaptic waveform at the granule cell to Purkinje cell synapse. *J Neurosci* **17**, 3425-35 (1997).
35. Zucker, R. S. & Regehr, W. G. Short-term synaptic plasticity. *Annu Rev Physiol* **64**, 355-405 (2002).
36. Habets, R. L. & Borst, J. G. Post-tetanic potentiation in the rat calyx of Held synapse. *J Physiol* **564**, 173-87 (2005).
37. Rosenmund, C. et al. Differential control of vesicle priming and short-term plasticity by Munc13 isoforms. *Neuron* **33**, 411-24 (2002).
38. Binzegger, T., Douglas, R. J. & Martin, K. A. A quantitative map of the circuit of cat primary visual cortex. *J Neurosci* **24**, 8441-53 (2004).
39. Deuchars, J., West, D. C. & Thomson, A. M. Relationships between morphology and physiology of pyramid-pyramid single axon connections in rat neocortex in vitro. *J Physiol* **478 Pt 3**, 423-35 (1994).
40. Douglas, R. J., Koch, C., Mahowald, M., Martin, K. A. & Suarez, H. H. Recurrent excitation in neocortical circuits. *Science* **269**, 981-5 (1995).
41. Gilbert, C. D. & Wiesel, T. N. Clustered intrinsic connections in cat visual cortex. *J Neurosci* **3**, 1116-33 (1983).
42. Markram, H., Lubke, J., Frotscher, M., Roth, A. & Sakmann, B. Physiology and anatomy of synaptic connections between thick tufted pyramidal neurones in the developing rat neocortex. *J Physiol* **500 (Pt 2)**, 409-40 (1997).
43. Peters, A., Jones, E.G. *Cellular Components of the Cerebral Cortex* (ed. Peters, A., Jones, E.G.) (Plenum Press, New York, 1984).
44. Thomson, A. M., West, D. C., Wang, Y. & Bannister, A. P. Synaptic connections and small circuits involving excitatory and inhibitory neurons in layers 2-5 of adult rat and cat neocortex: triple intracellular recordings and biocytin labelling in vitro. *Cereb Cortex* **12**, 936-53 (2002).
45. Debanne, D., Guerineau, N. C., Gahwiler, B. H. & Thompson, S. M. Action-potential propagation gated by an axonal I(A)-like K+ conductance in hippocampus. *Nature* **389**, 286-9 (1997).
46. Debanne, D., Kopysova, I. L., Bras, H. & Ferrand, N. Gating of action potential propagation by an axonal A-like potassium conductance in the hippocampus: a new type of non-synaptic plasticity. *J Physiol Paris* **93**, 285-96 (1999).
47. Cox, C. L., Denk, W., Tank, D. W. & Svoboda, K. Action potentials reliably invade axonal arbors of rat neocortical neurons. *Proc Natl Acad Sci U S A* **97**, 9724-8 (2000).
48. Koester, H. J. & Sakmann, B. Calcium dynamics associated with action potentials in single nerve terminals of pyramidal cells in layer 2/3 of the young rat neocortex. *J Physiol* **529 Pt 3**, 625-46 (2000).

*Department of Neurobiology, Kavli Institute for Neuroscience, Yale University School of Medicine, 333 Cedar Street New Haven, CT 06510 www.mccormicklab.org

49. Dorval, A. D., Christini, D. J. & White, J. A. Real-Time linux dynamic clamp: a fast and flexible way to construct virtual ion channels in living cells. *Ann Biomed Eng* **29**, 897-907 (2001).
50. Steriade, M., Timofeev, I. & Grenier, F. Natural waking and sleep states: a view from inside neocortical neurons. *J Neurophysiol* **85**, 1969-85 (2001).
51. Sanchez-Vives, M. V. & McCormick, D. A. Cellular and network mechanisms of rhythmic recurrent activity in neocortex. *Nat Neurosci* **3**, 1027-34 (2000).
52. Mainen, Z. F. & Sejnowski, T. J. Influence of dendritic structure on firing pattern in model neocortical neurons. *Nature* **382**, 363-6 (1996).
53. Mainen, Z. F., Joerges, J., Huguenard, J. R. & Sejnowski, T. J. A model of spike initiation in neocortical pyramidal neurons. *Neuron* **15**, 1427-39 (1995).

*Department of Neurobiology, Kavli Institute for Neuroscience, Yale University School of Medicine, 333 Cedar Street New Haven, CT 06510 www.mccormicklab.org